ELSEVIER

Characterization of air terminal device noise using acoustic 1-port source models

H. Rämmal, M. Abom*

The Marcus Wallenberg Laboratory for Sound and Vibartion Research, KTH, Teknikringen 8, S-100 44 Stockholm, Sweden

Abstract

A measurement method to characterize a standard air terminal device as an acoustic 1-port source has been tested and validated. The low-frequency noise generated by flow separation in the device and radiated to a reverberation room has been measured, together with pressure auto- and cross-spectra inside the connected duct. A 1-port source model with parameters derived from the in-duct data was then created. For the source strength part a scaling law was derived showing dipole dependence for the flow speed exponent. To validate the 1-port model and to prove its ability to predict flow noise generation, measurements were performed on a modified duct system.
© 2006 Elsevier Ltd. All rights reserved.

1. Introduction

As a result of interaction between the air flow and duct discontinuities flow-induced noise can reach significant levels in duct systems and become a limiting factor determining the minimum sound level. The sound field in a duct system depends on both the passive and active properties of the system. The passive properties are controlled by duct geometry, boundary conditions and the speed of sound which determine the sound propagation through the system, while the active properties define the acoustic sources in the system and describe how sound energy is generated [1]. To solve problems of noise reduction and to understand aerodynamic noise generation mechanisms, it is necessary to characterize noise sources. A source is commonly described by the physical quantities via which it interacts with the outside world. In the simplest case where an infinite space around the source can be assumed, the source can be characterized by its radiated acoustic power. This sound power-based description is the basis of most standards for the analysis of sound in ducts, e.g., see ASHRAE [2], and is valid in the high-frequency range. In general more complex source descriptions such as multiport models are needed [1], to correctly describe the interaction between a source and a duct system, which can occur in particular for low frequencies. Regarding the case studied here it will be suggested that an air terminal device (ATD), in the low-frequency (plane wave) region, can be modeled as an acoustic 1-port source. To the authors knowledge, this represents one of the first efforts to represent a flow generated source process as an active acoustic multiport.

---

*Corresponding author. Tel.: +46 8 790 7944; fax: +46 8 790 6122.

E-mail address: matsabom@kth.se (M. Abom).

The ATD investigated in this paper is a standard device typically mounted to the ventilation duct openings in buildings. Its purpose is to regulate and distribute the air flow in a room. Although the ATD studied is designed for ventilation systems used in buildings, the modeling approach suggested is applicable for ATDs in general, e.g., for the ventilation system in vehicles. Here, a recent paper on the aeroacoustics of automotive vents can be mentioned [3]. Just as the present paper this paper use the two-microphone technique to investigate the sound reflection, for the sound generation the focus is on the exterior while here both interior and exterior fields are investigated.

Following Lavrentjev [4] the source data of an acoustic 1-port, as a linear and time invariant system, can in the frequency domain be completely described by the source reflection coefficient and the source strength. In the present paper, the source impedance is first determined using the two microphone method [5]. As a second step, the source strength is determined by measuring the acoustic pressure spectrum with a known acoustic load connected to the duct inlet. In addition the sound power level, emitted from the ATD to a reverberant room, was determined using a standard measurement method (ISO 3747). All the experimental data obtained were at low Mach numbers ($M < 0.05$). In duct systems with low Mach numbers the dominating mechanism for flow generated sound is aero-acoustic dipoles created by fluctuating pressures in regions of flow separation [6]. In order to provide a prediction of the flow noise generation at different operating points a scaling law is derived. In the last part of the paper a new duct system connected to the given ATD is studied to validate the 1-port model.

2. Theory

The behavior of an acoustic 1-port (see Fig. 1) can in the frequency domain, be described by [1,4]

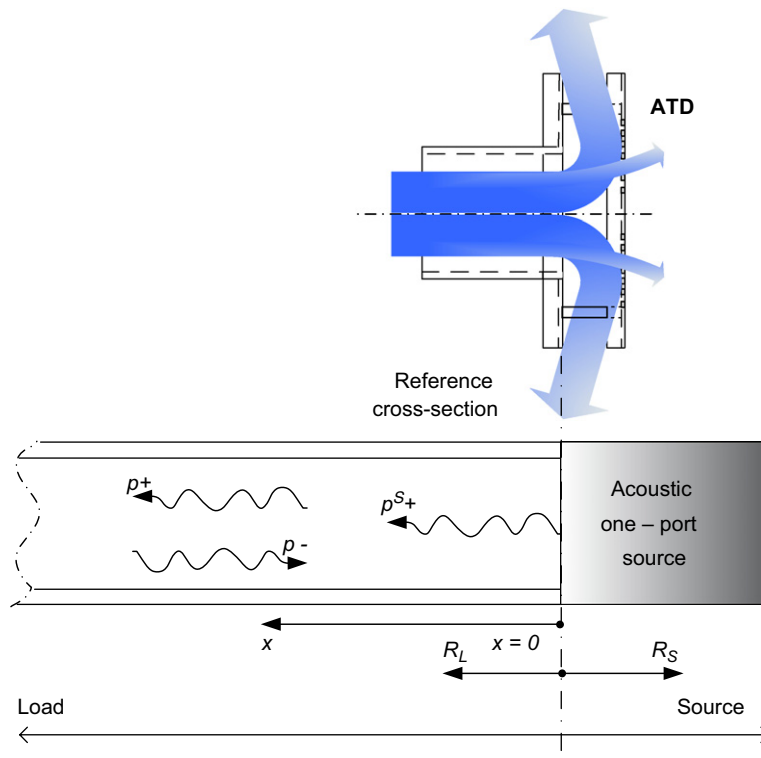$$p_+ = R_S p_- + p_+^S, \tag{1}$$

Fig. 1. Representation of an ATD, a device regulating the air flow at the end of a duct system, as an acoustic 1-port source.

where p_-, p_+ are traveling acoustic pressure amplitudes, R_S is the source reflection coefficient and p_+^S is the source strength.

The 1-port model can be used as long as the studied source process is linear, time invariant and the source term can be regarded as independent of the acoustic field. Following Bodén and Åbom [1] two basic approaches exist for the determination of the source data; methods *with* and *without* an external source. When possible to apply the methods with an external source are preferred and normally give a better result. Such a method will be applied here and is based on a two step procedure. First, the source reflection coefficient is determined using the external source and the two-microphone technique [5]. Then with the external source turned off or removed a known acoustic load is applied to determine the source strength.

2.1. Determination of the passive source data

Using the pressure signals from microphones 1 and 2 (Fig. 2) it is possible to separate left- and right-going waves and then to calculate the reflection coefficients and the source impedance. The plane wave acoustic pressures at microphones 1 and 2 can be written as [5]

$$p_1(f) = p_{1+}(f) + p_{1-}(f), \tag{2}$$

$$p_2(f) = p_{1+}(f)\exp(-ik_+s) + p_{1-}(f)\exp(ik_-s), \tag{3}$$

where p is the acoustic pressure, f the frequency, $k = 2\pi f/c$ the wavenumber, c the speed of sound, s the microphone separation, $-$ and $+$ denote the pressure waves propagating in neg. and pos. direction relative to the x-axis, $k_- = k/(1 - M)$, $k_+ = k/(1 + M)$ and M is the Mach number. Using the transfer function between the microphones 1 and 2 the acoustic reflection coefficient can be obtained [5]. The measurements of the transfer functions were done at different flow speeds both with the ATD and with a free termination (ATD valve removed). The reflection coefficient is defined as

$$R_S^r(f) = \frac{p_{1-}^e(f)}{p_{1+}^e(f)}, \tag{4}$$

where r denotes values measured at a reference point (microphone 1 cross-section) and p_-^e, p_+^e is the acoustic field generated by the external (loudspeaker) source. From Eqs. (2) to (4) it can be shown that [5]

$$R_S^r(f) = \frac{H_{12}^e - \exp(-ik_+s)}{\exp(ik_-s) - H_{12}^e}, \tag{5}$$
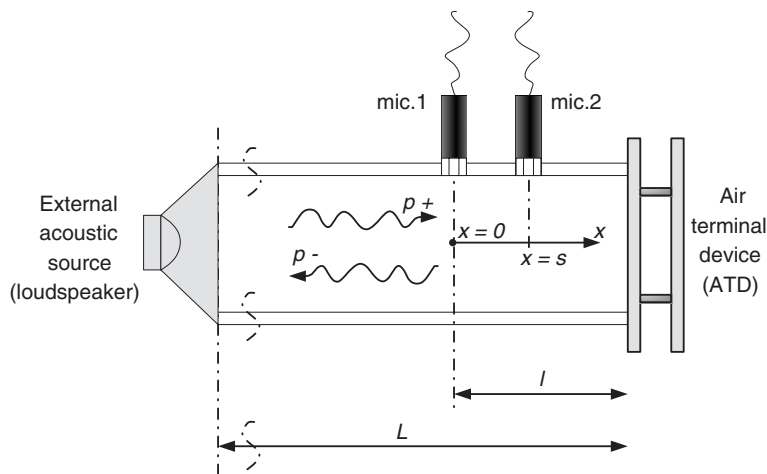

Fig. 2. Basic measurement configuration for the two-microphone method for impedance measurements. Determination of the source impedance.
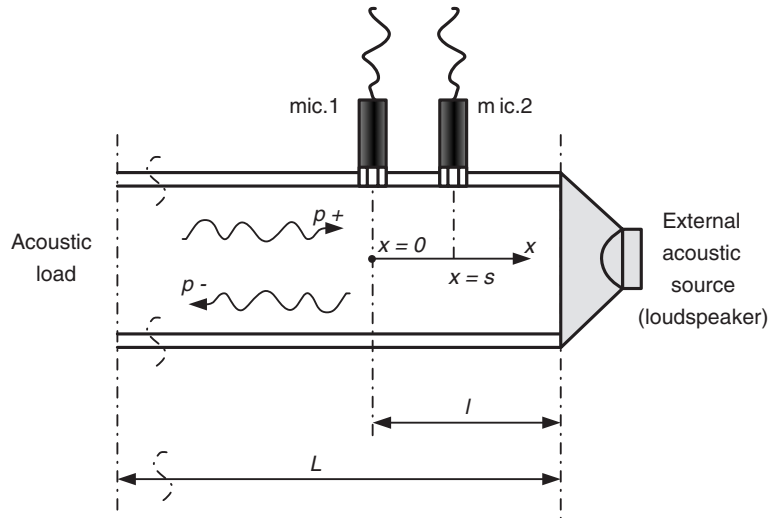
Fig. 3. Basic measurement configuration for the two-microphone method for impedance measurements. Determination of the acoustic load.

where $H_{12}^e = h_2/h_1$ is the transfer function from microphones 1 to 2 and $h_1 = p_1/e$ and $h_2 = p_2/e$ are the transfer functions between the microphone signals p_1, p_2, and the reference signal (here the electrical signal e driving the loudspeaker), respectively. A "single" microphone approach was used to avoid the phase calibration needed when two different microphones are used. Likewise, the load reflection coefficient (loudspeaker mounted instead of the ATD, see Fig. 3) can be obtained from

$$R_L^r(f) = \frac{p_{1+}^e(f)}{p_{1-}^e(f)} = \frac{H_{12}^e - \exp(ik_-s)}{\exp(-ik_+s) - H_{12}^e}. \tag{6}$$

In order to determine the acoustic properties of the ATD (at the outlet cross-section of the ATD, see Fig. 2), it is necessary to move all measured quantities, i.e., R_S^r, R_L^r to this location. This can be done by using the following equations:

$$R_S = R_S^r \exp(i(k_+ + k_-)l), \tag{7}$$

$$R_L = R_L^r \exp(-i(k_+ + k_-)l), \tag{8}$$

where l is the distance from the reference position (microphone 1 cross-section) to the desired cross-section (ATD).

When the source reflection coefficient is known the normalized acoustic impedance of the source Z_S is given by the equation

$$Z_S = \frac{1 + R_S}{1 - R_S}. \tag{9}$$

2.2. Determination of the active source data

As the second step, after the modifications of the test-rig used for impedance measurements, the source strength was determined. During the source strength measurements the external source was not in use and the ATD was acting like a source for the different flow speeds (see Section 3). To avoid additional flow noise creation, the loudspeaker unit was removed from the duct system.

In order to suppress effects of turbulence noise in the acoustic measurements, which can be a large problem especially for measurements on weak sources as in this case, two different microphone positions were used [4]. The source auto-spectrum was obtained from a measured sound pressure cross-spectrum G_{13} between microphones 1 and 3 (see Fig. 4). The microphones were flush mounted at the inner duct wall and
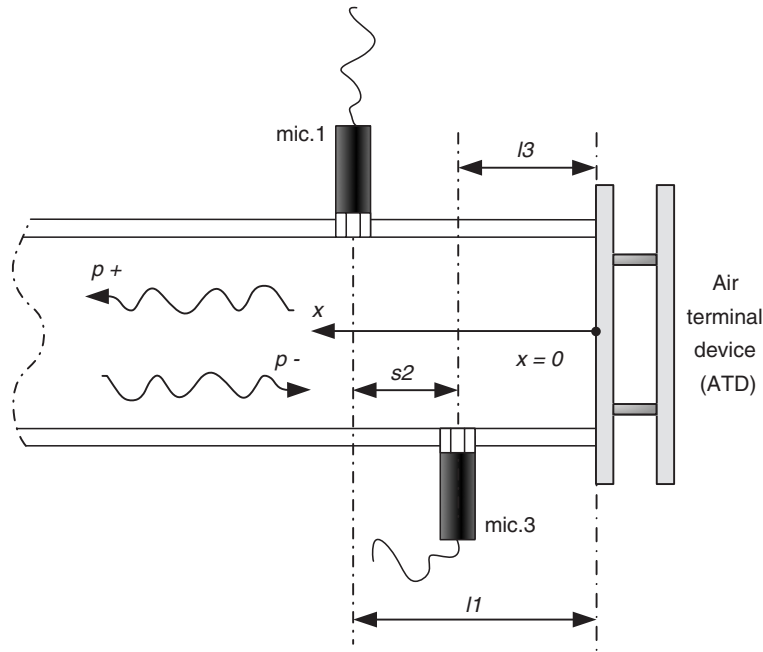
Fig. 4. Basic measurement configuration for source strength measurements.

microphone 3 was positioned to the opposite side of the pipe. Assuming that the two positions, say x_1 and x_3, are sufficiently separated so that local turbulent pressure fluctuations are uncorrelated, this approach will improve the measurement quality.

To derive the equation for the source strength p_+^S the load reflection coefficient, at the source cross-section R_L, is introduced in Eq. (1). As a result the following equation for the source strength is obtained:

$$p_+^S = p_+(1 - R_S R_L). \tag{10}$$

The pressure wave propagating in positive direction, at microphone 1 is given by

$$p_{1+} = \frac{p_1}{(1 + R_L^r)}. \tag{11}$$

To move the pressure p_{1+} to the assumed ATD source cross-section, the following equation is used:

$$p_+ = p_{1+} \exp(\mathrm{i}k_+ l_1), \tag{12}$$

where l_1 is the distance between microphone 1 and the source cross-section (see Fig. 4).

Using the Eqs. (10) and (12) gives

$$p_+^S = p_{1+} \exp(\mathrm{i}k_+ l_1)(1 - R_S R_L) \tag{13}$$

and if Eq. (13) is combined with Eq. (11), we obtain

$$p_+^S = \frac{p_1 \exp(\mathrm{i}k_+ l_1)(1 - R_S R_L)}{(1 + R_L^r)}, \tag{14}$$

where the load reflection coefficient at the microphone 1 cross-section is $R_L^r = R_L \exp(\mathrm{i}(k_+ + k_-)l_1)$. Now the source strength can be written in the following form:

$$p_+^S = \frac{p_1 \exp(\mathrm{i}k_+ l_1)(1 - R_S R_L)}{(1 + R_L \exp(\mathrm{i}(k_+ + k_-)l_1))}. \tag{15}$$

Eq. (15) could be used directly for the source strength measurements, but for turbulence noise suppression the second microphone (mic. 3), where the flow noise is assumed to be uncorrelated with the noise at

microphone 1, is additionally used and a cross-spectrum measurement is performed. To make a correction of the phase error between the microphones, the cross-spectrum G_{13} between the microphones 1 and 3 was measured twice, by switching microphone positions. The corrected cross-spectrum was then obtained from

$$G_{13cor} = \sqrt{G_{13} G_{13,switched}}. \tag{16}$$

The source auto-spectrum estimate $G_{SS} = E[p_+^S (p_+^S)^c]$ is finally obtained by using Eq. (14), and the cross-spectrum definition $G_{13} = E[p_1 p_3^c]$,

$$G_{SS} = \frac{G_{13cor} \exp(ik_+(l_1 - l_3))|1 - R_S R_L|^2}{(1 + R_L \exp(i(k_+ + k_-)l_1))(1 + R_L \exp(i(k_+ + k_-)l_3))^c}, \tag{17}$$

where the superscript c denotes a complex conjugated quantity and $E[\ ]$ denotes an ensemble average. Since the resulting auto-spectrum should be real-valued only the real part of the estimate in Eq. (17) will be considered.

2.3. Sound power radiated

Of interest in practice is the determination of the sound power radiated from an ATD unit. When the 1-port source data is known the resulting volume flow q in the opening will create a monopole type of source. The volume flow in the opening can be written as $q = S \cdot (u_+ + u_-)$, where u is the acoustic velocity in the $\pm x$-direction (see Fig. 4) and S is the cross-sectional area of the duct. It is known that $u_+ = (p_+/\rho c)$, $u_- = -(p_-/\rho c)$, using Eq. (10) this implies

$$q = \frac{p_+^S S(1 - R_L)}{\rho c(1 - R_S R_L)}, \tag{18}$$

where ρ is the density. For sufficiently low frequencies and small Mach-numbers, the radiation from the ATD will be dominated by a monopole [7,8], i.e., the first non-zero term in a multipole expansion of the fluctuating field at the opening. As shown by Bechert [7], the dipole contribution will be negligible under these conditions. This implies that if the acoustic volume flow q at the ATD is known then the radiated power is

$$W_{rad} = \frac{\rho c k^2 |q|^2}{4\pi}. \tag{19}$$

Combining this with Eq. (18) leads to

$$W_{rad} = \frac{\pi^3 f^2 d^4 |1 - R_L|^2 G_{SS}}{16 c^3 \rho |1 - R_s R_L|^2}, \tag{20}$$

where $S = \pi d^2 / 4$ and d the duct diameter has been inserted. Expressing this as levels using the normal reference values gives

$$L_W = L_S + 10 \log_{10} \left(\frac{\pi^3 f^2 d^4 |1 - R_L|^2}{16 c^3 \rho |1 - R_S R_L|^2} \right) + 26, \tag{21}$$

where $L_S = 10 \log_{10}(G_{SS}/p_{ref}^2)$ and $p_{ref} = 20 \,\mu Pa$.

2.4. A scaling law for the source strength

To enable source data measured at one operating condition to be used at other operating points (flow speeds) a scaling law is necessary. As observed in earlier investigations, e.g., Lavrentjev [4], the passive part of the source data is often weakly dependent on the flow speed. Therefore, it is mainly of interest to find a scaling law for the source strength. Similar to earlier works, e.g., Nelson and Morfey [6], a scaling formula for the in-duct plane wave sound power produced by flow separation will be used:

$$\frac{G_{SS}}{\rho c} = \rho U^3 M^\alpha F(St), \tag{22}$$

where U is the mean flow speed, α depends on the aero-acoustic source type, $F(St)$ is a dimensionless source-spectrum depending on a Strouhal number, $St = fd/U$, f is the frequency and d is the duct diameter. When writing down the power in the plane wave in Eq. (22), the effect of the mean flow has been omitted. The scaling law in Eq. (22) is general and only assumes that a fraction of the kinetic energy in the flow is converted into sound. It is therefore not explicitly based on a compact dipole source as the scaling law used by Nelson and Morfey [6]. For the ATD studied the experiments show that the best collapse is obtained with $\alpha = 0$. This corresponds to a flow speed exponent of 3 for the flow separation source known to be of dipole type. The expected speed exponent 4 for an aeroacoustic dipole in the plane wave range [6], is obtained after integrating Eq. (22) over, e.g., a one-third octave band.

3. Measurements

Measurements were performed on a standard rectangular ATD shown in Fig. 5 and on a circular orifice (with inner diameter of 73 mm, see Fig. 6) mounted to the end of the test duct. Three different measurement setups were used in the experiments. First in duct measurements were performed with an external sound source (loudspeaker) for source impedance determination, using the two-microphone technique, see Figs. 7 and 8. Secondly, the source strength was measured using the same rig but with the loudspeaker section removed, see Figs. 9 and 10. Thirdly, measurements were performed, according to the ISO 3747 standard, for radiated sound power emitted from the ATD to a reverberant room, see Figs. 11 and 12.

To create a flow in the duct, having an inlet in an anechoic room and an outlet connected to the ATD under study and located in a reverberation room, an axial fan was used to pressurize the anechoic room,
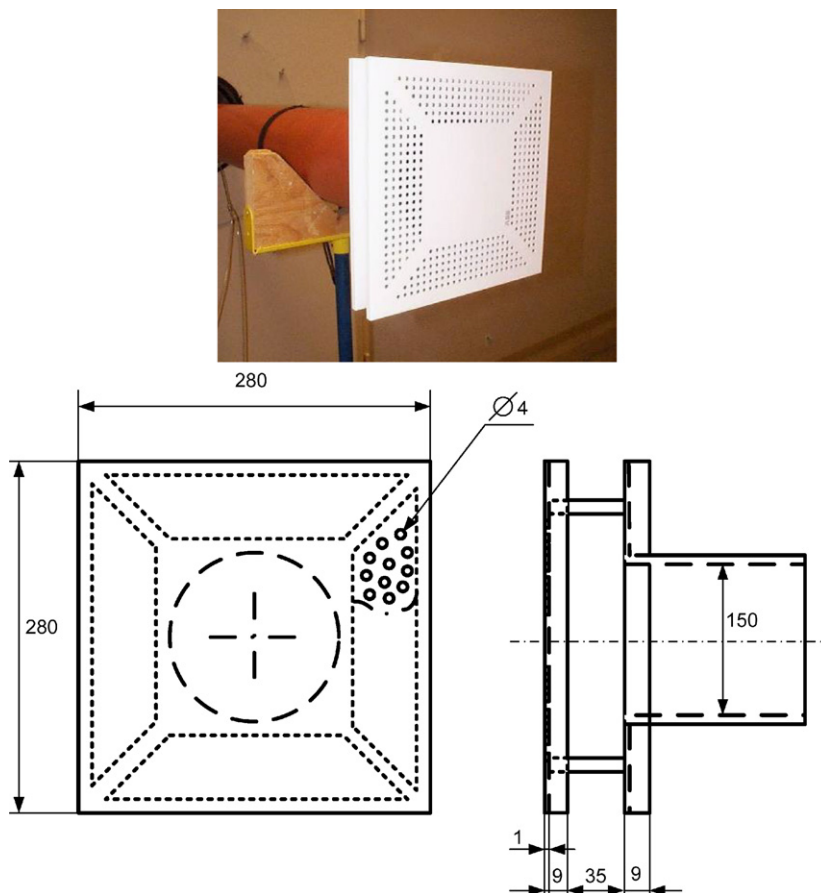

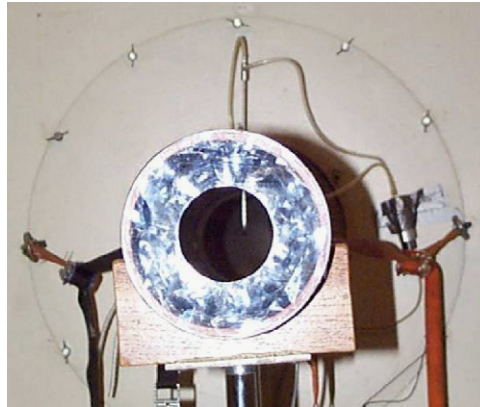Fig. 5. Photo and drawing (units in mm) of the standard ATD used in the experiments.

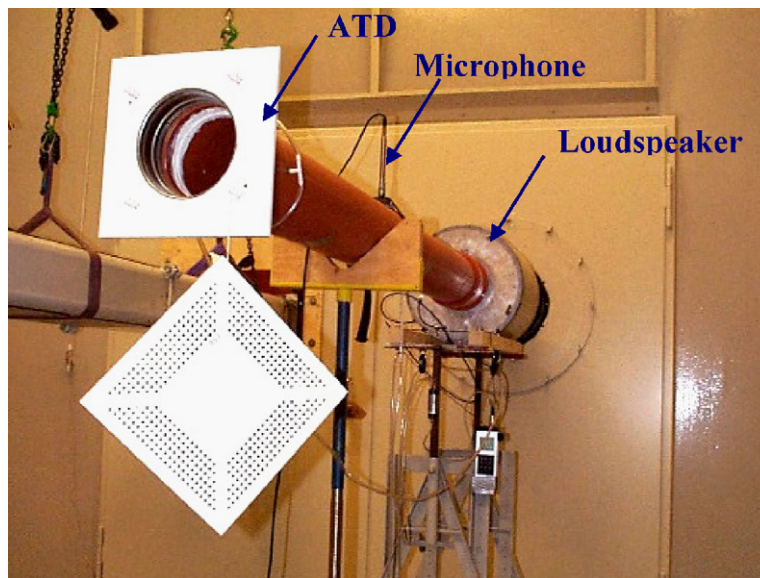Fig. 6. Photo of the circular orifice used in the experiments.

Fig. 7. Photo of the experimental setup for source impedance measurements.

see e.g. Fig. 8. The return flow of the air was through a third room with a system of silencers. The test duct consisted of a glass fiber conical inlet pipe and of PVC test pipes with circular cross-section and an inner diameter of 150 mm. For the in-duct acoustic pressure measurements 1/4-in condenser microphones (Brüel & Kjaer 2670 and Norsonic 1245) were used. In order to determine the flow speed in the duct system a Pitot-tube connected to an electronic micro-manometer was mounted in the duct, see e.g. Fig. 8. The static air pressure drop across the ATD was also measured using the same micro-manometer. As an external noise source for the impedance measurements, a loudspeaker positioned in the duct, was used. The loudspeaker was driven by a sound generator through a power amplifier and an equalizer. The signal acquisition was performed by a four-channel digital Fourier analyzer (Siglab 20-42) connected to a PC. The sound power measurements (according to ISO 3747) in the reverberation room (see Figs. 10–11) were performed using a 1/2-in microphone fixed to a rotating microphone support. The reference sound power was created by a calibrated fan-type sound source (Brüel & Kjaer 4204) positioned at the location of the ATD in the reverberation room.

Using the two-microphone method, the total error in calculated quantities from all disturbances will be smallest in a region around $ks = \pi/2$, where k is the wavenumber, and s is the separation of microphones 1
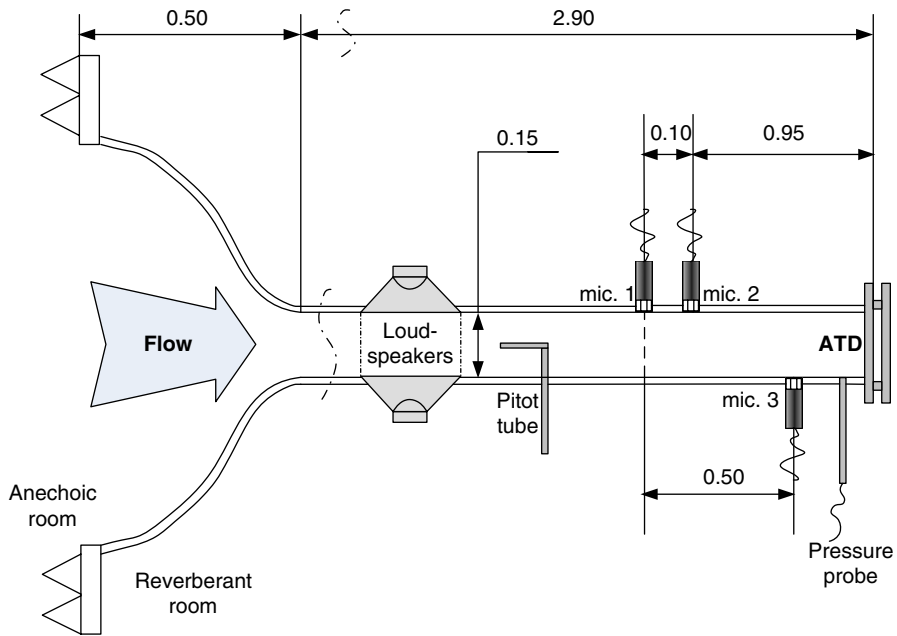
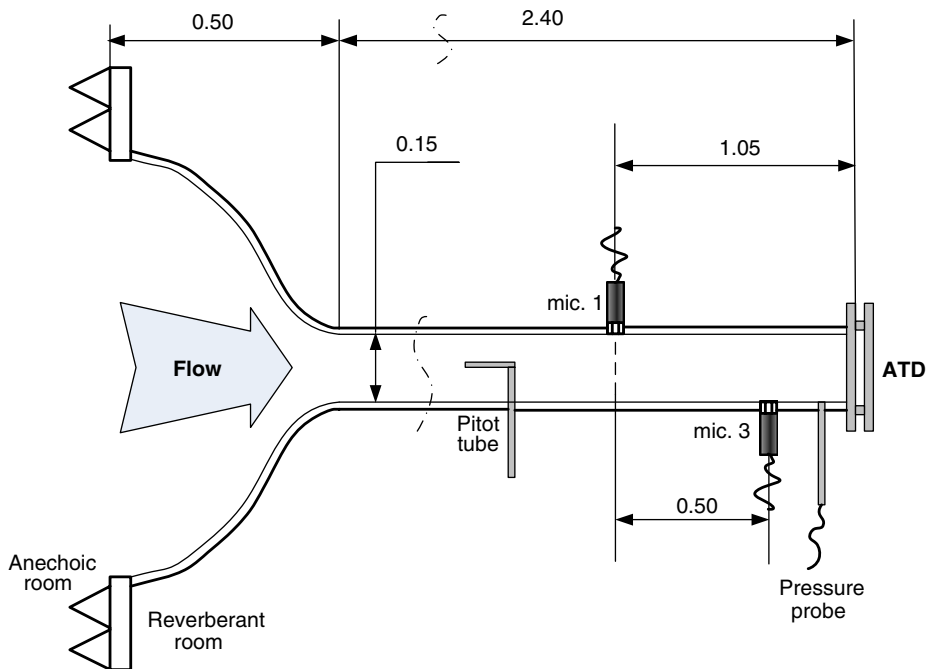Fig. 8. Layout of the rig for source impedance measurements. All units are in (m).

Fig. 9. Layout of the rig for source strength measurements. All units are in (m).

and 2 (see Fig. 2). If we restrict the two-microphone method to the region around $0.1\pi < ks < 0.8\pi$, the total error in the calculated quantities will at the most be a factor 10 times the error around $ks = \pi/2$ [5]. For the impedance measurements two different microphone separations were chosen: $s1 = 0.1\,\text{m}$ for frequencies from 175 Hz to the first cut-on frequency, and $s2 = 0.5\,\text{m}$ to cover a frequency region from 33 up to 175 Hz. The first
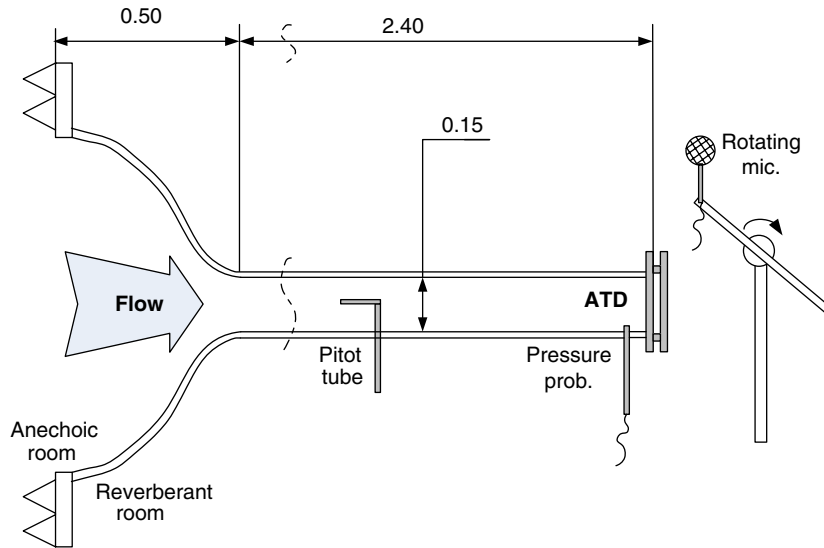
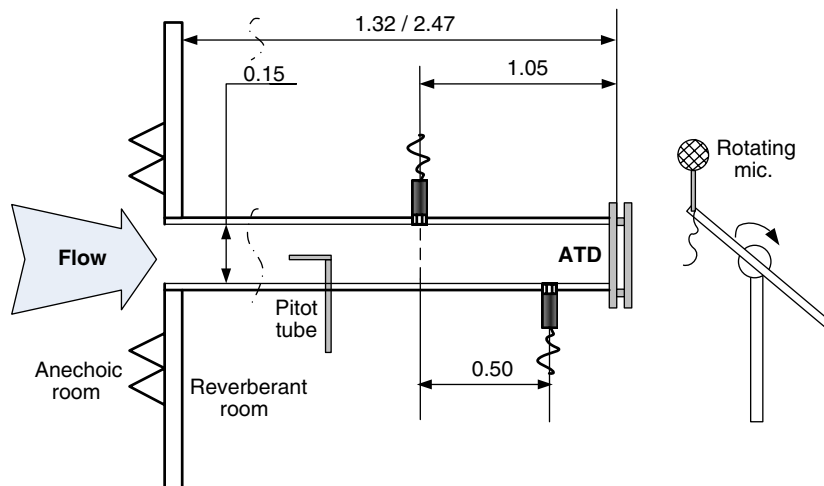Fig. 10. Layout of the rig for the radiated sound power measurements. All units are in (m).

Fig. 11. Layout of the rig for the validation measurements. All units are in (m). Note, that two different lengths were used 1.32 and 2.47 m.

cut-on frequency of the duct with an inner diameter $d = 0.146$ m was around 1400 Hz ($c = 343$ m/s). For the source strength measurements a microphone separation $s2 = 0.5$ m between microphone 1 and 3 (see Fig. 4) was used. A frequency resolution for the FFT—system of 1.25 Hz was chosen for the measurements. A relatively large number of averages (400 for the source and load impedance or alternatively the reflection coefficient measurements and for the source strength measurements, 250 for emitted sound power measurements) were used to achieve a good suppression of flow noise and to reduce the random error in the measurements.

At the real operating conditions the flow speed in the duct before the ATD is typically around 5 m/s. At this low speed the flow noise production is relatively small making accurate measurements difficult. One alternative is then to measure with higher flow velocities and use a scaling law to calculate the source data at the appropriate speed. In order to obtain data to derive a scaling law acoustic measurements were done for three different flow speeds: $U_1 = 8.2$ m/s, $U_2 = 12.3$ m/s and $U_3 = 16.4$ m/s.
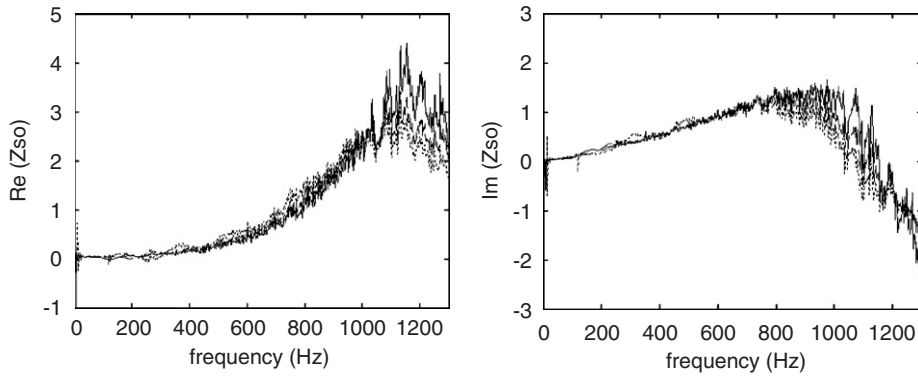
Fig. 12. The real and imaginary parts of the source impedance of the ATD; $U = 8.2\,\text{m/s}$ (solid), $U = 12.3\,\text{m/s}$ (long dash), $U = 16.4\,\text{m/s}$ (short dash).

Table 1
The pressure loss coefficient of the air terminal device

Flow velocity, v (m/s)	Pressure difference, Δp (Pa)	Pressure loss coefficient, CL
8.2	42.1	0.42100
12.3	94.8	0.42133
16.4	165.5	0.41375
		Average CL 0.41869

The pressure drop Δp across the ATD was measured for all the three flow speeds. The aim of this experiment was to determine a pressure loss coefficient C_L for the ATD. Using the following equation:

$$\Delta p = \frac{1}{2}\rho U^2 C_L, \tag{23}$$

the pressure loss coefficient can be derived. A value close to 0.42 was found from these tests, see Table 1.

For validation of the source model additional measurements were done with a modified duct system, having the same inner diameter but no conical inlet part (see Fig. 11). Both in-duct (cross-spectra) and reverberant room measurements (sound power) were performed. Two different flow velocities were chosen for the validation measurements; $U_1 = 7.0$ and $U_2 = 12.0\,\text{m/s}$. The reflection coefficients R_L for the conical inlet of the duct system and for the flanged inlet of the validation duct were determined experimentally. This was done in a separate measurement with the loudspeaker and microphone positions interchanged as compared to Fig. 8 and applying the two-microphone method.

4. Results and discussion

The measured (normalized) source impedances for the ATD (Fig. 12) show only a small dependence on flow speed up to 800–1000 Hz. For low frequencies the main effect of the flow will be related to dissipation [7,8] of acoustic energy, which can be related to the pressure drop over the ATD. From Refs. [9,10] it follows that the flow induced (normalized) acoustic resistance is given by

$$R_{\text{flow}} = MC_L. \tag{24}$$

This can be compared with the (normalized) radiation resistance which, assuming a monopole type of radiation, is given by

$$R_{\text{rad}} = \frac{(kd)^2}{16}. \tag{25}$$

From the model for low-frequency sound radiation from pipe openings with flow [8], it follows that R_{flow} and R_{rad} act as if they are in series. For the case studied here with a Mach number less than 0.05 and $C_L = 0.42$, we have $R_{\text{flow}} \leqslant 0.021$, so the radiation resistance will then dominate for frequencies above 200–300 Hz.

Results for the source strength auto-spectrum are shown in Fig. 13. Fig. 14 shows the coherence between microphones 1 and 3, used to determine the source strength according to Eq. (17). In Fig. 15, the collapse of all
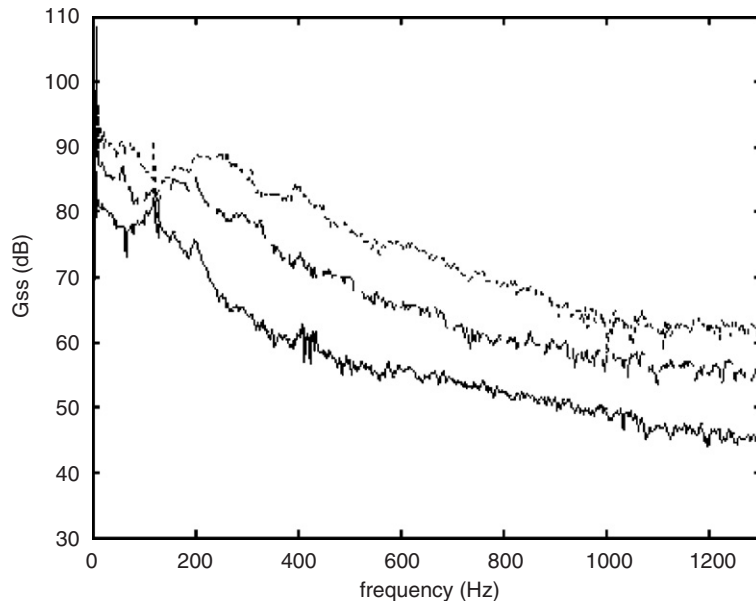

Fig. 13. The source strength of the air terminal device from in-duct measurements; $U = 8.2\,\text{m/s}$ (solid), $U = 12.3\,\text{m/s}$ (long dash), $U = 16.4\,\text{m/s}$ (short dash).
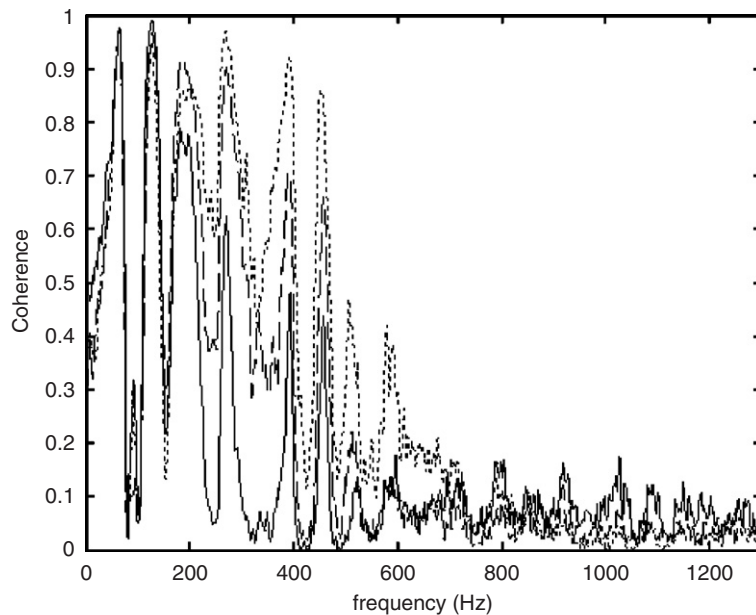

Fig. 14. The coherence between the two-microphones (1 and 3) used for the source strength measurements of the ATD; $U = 8.2\,\text{m/s}$ (solid), $U = 12.3\,\text{m/s}$ (long dash), $U = 16.4\,\text{m/s}$ (short dash).
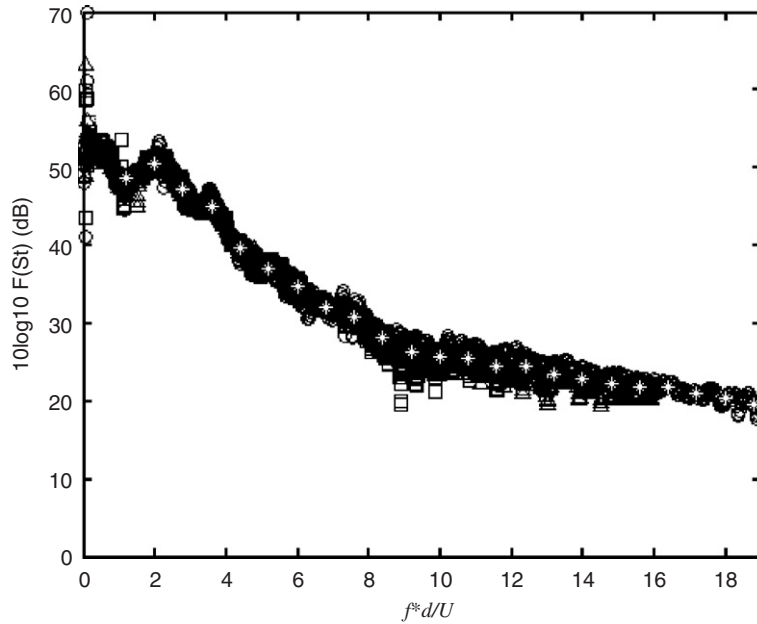
Fig. 15. Air terminal device: data collapse for the Strouhal number-dependent source spectrum F in Eq. (22); $\circ$ the source strength based on in-duct measurements, $U = 8.2$ m/s, $\triangle$ the source strength based on in-duct measurements, $U = 12.3$ m/s, $\square$ the source strength based on in-duct measurements, $U = 16.4$ m/s, * the best fit source model used in the validation.
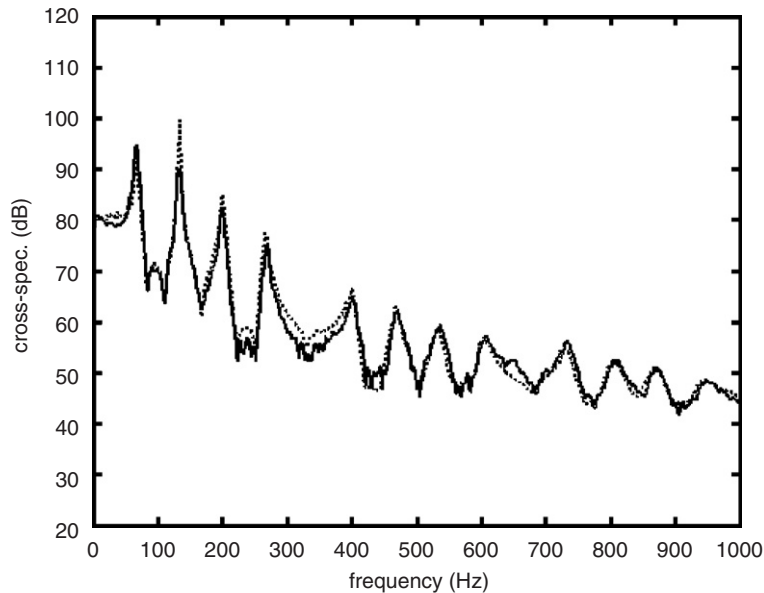

Fig. 16. The cross-spectrum G_{13} from the air terminal device with 7.0 m/s flow speed in the validation duct system (2.47 m); measurements (full line), prediction (dotted line).

the source strength data is shown, based on the scaling law in Eq. (22) with $\alpha = 0$, which was found to give the best fit. The scatter ("black region") around the best fit points is a measure of the standard deviation, which is of the order 3 dB. The α value found will create a flow speed exponent of 4 when integrated over all frequencies or over a frequency band with constant relative band-width, e.g., a 1/3-octave band. This value corresponds to a ducted aero-acoustic dipole in the plane wave range [6].

To validate the source model, including the scaling law for the source strength, the modified duct described above was used. In Figs. 16 and 17, examples for the prediction of the pressure cross-spectrum (G_{13}) are shown. As can be seen the agreement for the in-duct case is good with a deviation of typically less than 2 dB up to about 1000 Hz. In Figs. 18 and 19, examples for the prediction of the radiated sound power (Eq. (21)) are shown in 1/3-octave bands. Here, the agreement is not as good as for the in-duct case.
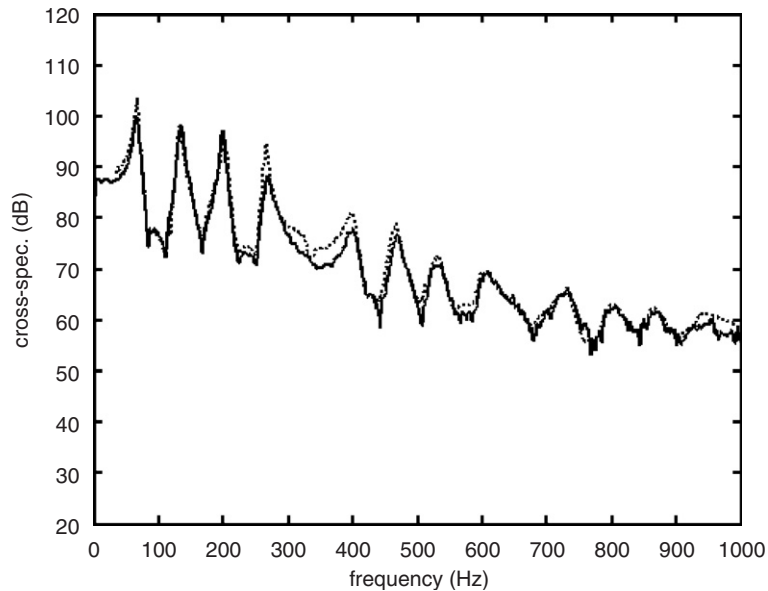

Fig. 17. The cross-spectrum G_{13} from the air-terminal device with 12.0 m/s flow velocity in the validation duct system (2.47 m); measurements (full line), prediction (dotted line).
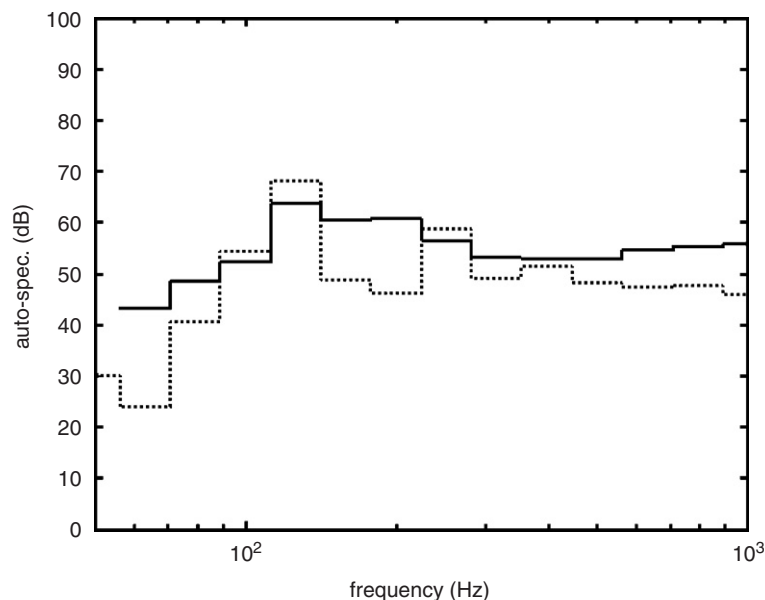

Fig. 18. Sound power spectrum (1/3-octave bands) in the reverberation room from the air terminal device with 7.0 m/s in the validation duct system (2.47 m); measurements (full line), prediction (dotted line).
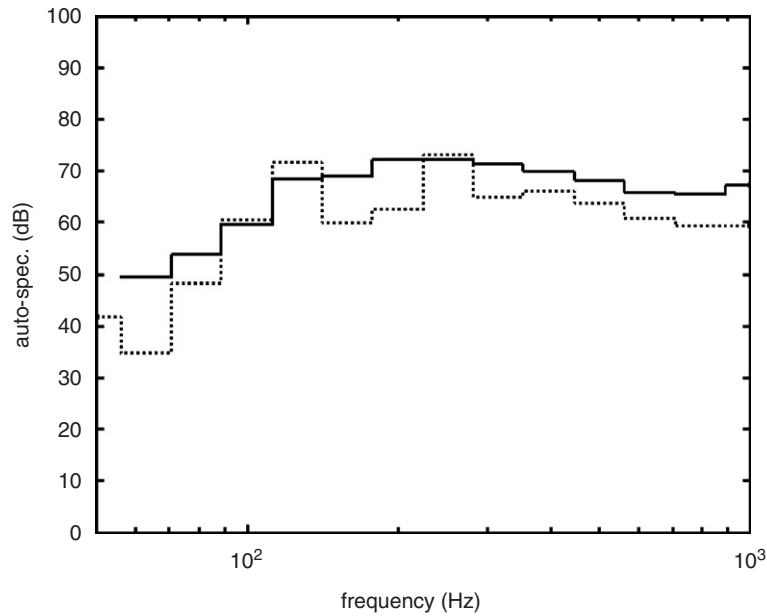
Fig. 19. Sound power spectrum (1/3-octave bands) in the reverberation room from the air terminal device with 12.0 m/s in the validation duct system (2.47 m); measurements (full line), prediction (dotted line).
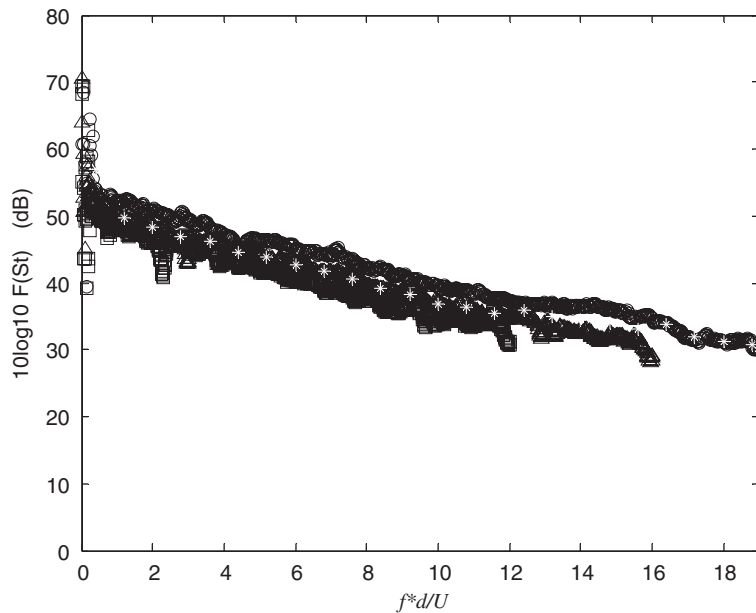

Fig. 20. Orifice constriction: Data collapse for the Strouhal number dependent source spectrum F in Eq. (22); $\circ$ the source strength based on in-duct measurements, $U = 8.2$ m/s, the source strength based on in-duct measurements, $U = 12.3$ m/s, the source strength based on in-duct measurements, $U = 16.4$ m/s, the averaged source model used in the validation.

In order to investigate the reason for the less good agreement for the radiated sound power the same source characterization procedure was performed with a simplified ATD, an orifice plate with a circular hole, Fig. 6. The dimensionless source spectrum for the orifice plate is shown in Fig. 20 and an example of the resulting radiated power is shown in Fig. 21. As can be seen the agreement is much better for this case than for the ATD unit. This and other tests led to the conclusion that the resulting dipole generated by an obstruction at a duct
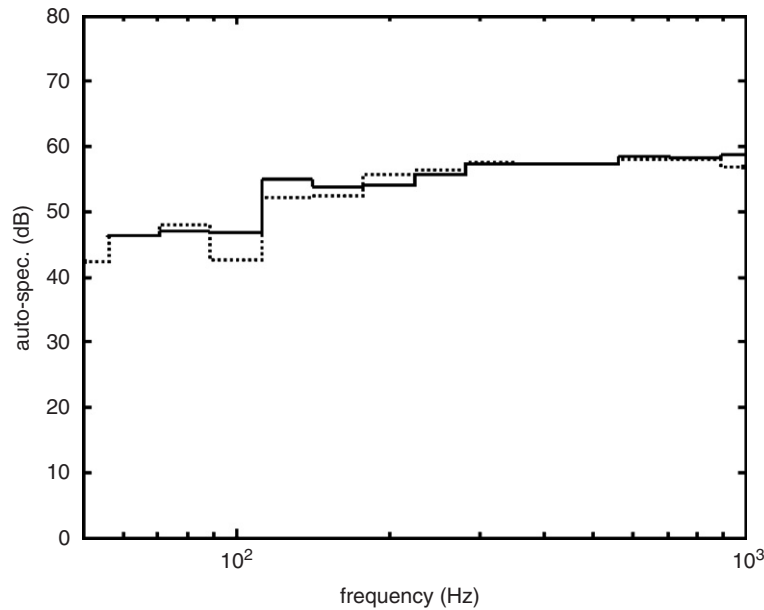
Fig. 21. Sound power spectrum in 1/3-octave bands in the reverberation room from the orifice constriction with 7.0 m/s in the validation duct system; measurements (full line), prediction (dotted line).

opening often has non-axial components. These components are created when the obstruction deflects the flow from the axial direction by the fluctuating part of the external force components needed for the deflection. When the source data is determined inside the duct only the axial (along x) component of the dipole will excite a plane wave field. The source data determined inside the duct will therefore only contain information about this component. For the outside radiation a 3-D sound field exists and all dipole components, axial and non-axial, can play a role. Also since for the ATD studied here the source is located just outside the duct opening, around 1/10 of a wavelength at 1 kHz, the full axial dipole strength will not excite the sound field inside the duct. This effect together with the effect of non-axial dipoles creates a tendency to underestimate the radiated sound based on in-duct (plane wave) source data. It can be noted that the discussion above is in accordance with results presented in the paper by Heller and Widnall [11].

In conclusion, the 1-port model can be used to calculate the external field generated by the axial component of a dipole at the duct opening. If non-axial components exist they are uncoupled to the plane wave inside the duct [11] and their resulting external fields can, for low frequencies, be calculated by only considering the external problem. The resulting fields can then be superimposed on the solution for the axial component to obtain the total external field.

5. Summary and conclusions

This paper represents an effort to use 1-port models to characterize low frequency (plane wave) flow generated sound in ducts. This procedure should work as long as the source process is unaffected by the acoustic field. This is consistent with the basic assumption used when writing down the source term in Lighthills famous equation. Therefore, it holds in many cases with the exception of situations where strong flow-acoustic feedback occurs, e.g., whistles. In the paper this approach has been tested and found to predict well the in-duct sound produced by an ATD. In the experimentally derived scaling law a flow speed dependence of 3 was found for the narrow band spectra, corresponding to a dipole-like behavior of the source in the plane wave range. The present work together with the earlier work by Nygård [9] also summarized in Ref. [10], represents to the authors knowledge the first efforts to apply active multiport models to describe flow generated noise. In these earlier works also done at KTH [9,10] flow generated noise from duct bends was studied and modeled using an active 2-port.

The use of 1- and 2-port models is of importance for modeling the low-frequency plane wave range in duct systems. This range is of particular interest to study resonance and standing wave effects that significantly can affect the acoustic output. An interesting future continuation of this work would be to try to establish methods to estimate 1- and 2-port source data directly from CFD calculations. Since the passive part of the source data often is weakly affected by the flow it could be sufficient "only" to estimate the (active) source strength part.

References

[1] H. Bodén, M. Åbom, Modeling of fluid machines as sources of sound in duct and pipe systems, *Acta Acustica* 3 (1995) 1–12.

[2] ASHRAE, Sound and Vibration Control, *2003 ASHRAE Applications Handbook*, ASHRAE Inc., Atlanta, 2003 (Chapter 47).

[3] S. Guérin, E. Thomy, M.C.M. Wright, Aeroacoustics of automotive vents, *Journal of Sound and Vibration* 285 (2005) 859–875.

[4] J. Lavrentjev, Multi-port Models for Source Characterization of Fluid Machines. Doctoral Thesis, TRITA-FKT-9828. ISSN 1103-470X. The Marcus Wallenberg Laboratory, KTH, 1998.

[5] M. Åbom, H. Bodén, Error analysis of two-microphone measurements in ducts with flow, *Journal of Acoustical Society of America* 83 (1988) 2429–2438.

[6] P.A. Nelson, C.L. Morfey, Aerodynamic sound production in low speed flow ducts, *Journal of Sound and Vibration* 79 (1981) 263–286.

[7] D.W. Bechert, Sound absorption caused by vorticity shedding demonstrated with a jet flow, *Journal of Sound and Vibration* 70 (1980) 389–405.

[8] M.S. Howe, The dissipation of sound at an edge, *Journal of Sound and Vibration* 70 (1980) 407–411.

[9] S. Nygård, Low Frequency Sound in Duct Systems. Lic. Tech Thesis, TRITA-FKT-0057, ISSN 1103-470X, The Marcus Wallenberg Laboratory, KTH, 2000.

[10] H. Gijrath, S. Nygård, M. Åbom, Modeling of flow generated sound in ducts. ICSV 8, Hong Kong, *Paper No. 578*, 2001.

[11] H.H. Heller, S.E. Widnall, Sound radiation from rigid flow spoilers correlated with fluctuating forces, *Journal of Acoustical Society of America* 47 (1970) 924–936.